

Research paper

Four new Cu^I/Ag^I-based coordination compounds containing 2-mercapto-5-methyl-1,3,4-thiadiazole: Synthesis, crystal structures and fluorescence properties

Ying Geng^a, Wen Zhang^a, Jiang-Feng Song^a, Rui-Sha Zhou^{a,*}, Wei-Zhou Jiao^{b,*}

^a Department of Chemistry, North University of China, Taiyuan, Shanxi 030051, PR China

^b Shanxi Province Key Laboratory of Hige-Oriented Chemical Engineering, North University of China, PR China



ARTICLE INFO

Keywords:

Coordination polymers
Crystal structure
Fluorescence
Organic sulfur
Sensing

ABSTRACT

Effectively constructing Cu^I/Ag^I-based coordination polymers containing Hmthd ligands is a challenging work, here, four new coordination compounds [Cu(Hmthd)₂Cl]_n (1), [Cu₃(mthd)₂Br]_n (2), [Ag(mthd)]_n (3) and [Ag₂(mthd)]_n (4) have been obtained by reactions of the corresponding metal salts and 2-mercapto-5-methyl-1,3,4-thiadiazole (Hmthd) ligand under solvothermal conditions. All the compounds were fully characterized by single-crystal X-ray diffraction, elemental analysis, IR spectrum, thermalgravimetric analysis and powder X-ray diffraction. Compound 1 is a mononuclear coordination compound, in which two neutral Hmthd molecules and CuCl unit are coplanar. In compound 2, the anionic [CuBr(mthd)]₂²⁻ units and one-dimensional coplanar cationic {[Cu₂(mthd)]⁺}_n chains are connected to each other to form a two-dimensional layered structure. In compound 3, two different one-dimensional puckered [Ag(mthd)]_n chains are connected to each other to form a two-dimensional irregular layered structure, in which a (AgS)_n chain constructed by staggered Ag₃S₃ rings is observed. Compound 4 is a two-dimensional double layer coordination framework containing a two-dimensional inorganic (Ag₂IS)_n double layer. Compound 4 shows the apparent yellow emission with the maximum at 551 nm while exciting at 333 nm, and displays sensitive luminescence quenching response to nitrobenzene with quenching constant (K_{sv}) of 5.07 × 10³ M⁻¹ and detection limit of 5.33 × 10⁻⁶ M. This research provides a new strategy to construct the Cu^I/Ag^I-based coordination compounds containing Hmthd ligands with extended structures through the synergistic effect of (mthd)⁻ and halide ions.

1. Introduction

Luminescent coordination compounds are a rapidly burgeoning class of crystalline materials which show great potential of a broad range of applications such as light emission, sensitive sensor, photo-catalysis, and so on [1–11]. Thus far, especially precious metal species such as Re^I, Au^I, Os^{II}, Pt^{II}, Ir^{III} [12–14], lanthanide ions with narrow and characteristic 4f–4f transitions together with transition metals with d¹⁰ electronic configurations are often utilized to construct the target luminescent coordination compounds [15–20]. Of particular interests are Cu^I/Ag^I-based coordination compounds with d¹⁰ electronic configurations, which are a developing class of luminescent materials based on an inexpensive and abundant metal sources as well as their remarkable luminescent performances. A typical strategy to synthesize Cu^I/Ag^I-based compounds usually requires the satisfactory choice of coordinating ligands, for

example, organic amine, organo-phosphine and organic-sulfur ligands are frequently used to construct the targeted compounds with novel structures and excellent properties [21–41]. Compared with organic amines and organophosphines, the sulfur atoms on organosulfur ligands display richer coordination modes and stronger bonding ability to match metal orbitals together with various in situ ligand/metal redox reactions [27,42–44]. Therefore, the controlled syntheses of organosulfur-based coordination compounds arouse widespread interests due to their structural diversity and potential applications such as sensing, heterogeneous catalysis and biological anti-bacterials [30,36].

mercapto-5-methyl-1,3,4-thiadiazole (Hmthd) is a typical multi-dentate five-membered heterocyclic compound which contains two heterocyclic nitrogen, one heterocyclic sulfur and one sulfhydryl group. Hmthd ligand has obvious advantages in the construction of

* Corresponding authors.

E-mail addresses: rszhou0713@nuc.edu.cn (R.-S. Zhou), zbdxjwz@nuc.edu.cn (W.-Z. Jiao).

<https://doi.org/10.1016/j.ica.2021.120596>

Received 17 July 2021; Received in revised form 16 August 2021; Accepted 26 August 2021

Available online 8 September 2021

0020-1693/© 2021 Elsevier B.V. All rights reserved.

the coordination compounds: (1) the two nitrogen and one sulfur of thiadiazole ring together with the introduced sulfhydryl group can be used as chelating ligands or bridging ligands to coordinate with metal ions; (2) the large-size sulfur can interact with metal ions through various coordination modes ranging from μ_1 to μ_4 , and its 3p orbitals show strong coordination ability to match metal orbitals, as result in the formation of multi-nucleus clusters or high-dimensional structures [43]; (3) Hmthd ligand shows a thione-thiol ($-\text{N}=\text{C}-\text{SH} \leftrightarrow -\text{NH}-\text{C}=\text{S}$) tautomeric transformation, resulting in the diversity of coordination modes. As far as we know, most of the reported compounds based on Hmthd or (mthd)⁻ were zero-dimensional (0 D) mononuclear compounds through the assembly of Hmthd and transition metal ions such as Ni²⁺, Cu²⁺, Zn²⁺, Cd²⁺, Hg²⁺ [45] or main metal ions Pb²⁺ [46], Sn⁴⁺ [47], and only Me₃Sn[S(C₃H₃N₂S)] displayed one-dimensional (1 D) polymeric chain [47]. Notably, the Cu^I/Ag^I-based compounds containing Hmthd ligands are less reported, therefore, effectively constructing Cu^I/Ag^I-based coordination compounds containing Hmthd ligands with extended structures is a challenging work.

According to hard-soft-acid-base theory, Cu^I/Ag^I belonging to soft acids should easily coordinate with soft bases such as S atom in organic sulfur ligands and obtain the targeted coordination compounds. In addition, considering that Cu^I/Ag^I ions have good binding ability with halogen ions, the introduction of halogen ions can effectively adjust the diversity of the target structures. Herein, we successfully synthesize four new coordination compounds through the synergistic interactions of (mthd)⁻ and halide ions, [Cu(Hmthd)₂Cl]_n (1), [Cu₃(mthd)₂Br]_n (2), [Ag(mthd)]_n (3) and [Ag₂(mthd)]_n (4), (Hmthd = 2-mercapto-5-methyl-1,3,4-thiadiazole). All the compounds were fully characterized by single-crystal X-ray diffraction, elemental analysis, IR spectrum, thermalgravimetric analysis and powder X-ray diffraction. Compound 1 is a 0 D mononuclear compound while compounds 2–4 show two-dimensional (2 D) layered structures, the results show introduction of halogen ions finely modulate the structural features of the target compounds. The fluorescence properties of compound 4 in the solid state and in various solvent molecules have also been investigated, displaying highly luminescence quenching response to nitrobenzene (NB).

2. Experimental

2.1. Materials and physical measurements

All reagents and solvents were commercially available and used as received without further purification. Elemental analysis (C, H and N) was performed on a Perkin-Elmer 240C elemental analyzer. Infrared (IR) spectra were obtained with KBr pellets on a Perkin Elmer Spectrum One FTIR spectrometer in the range of 4000–400 cm⁻¹. Powder X-ray diffraction (PXRD) patterns of the samples were recorded by a RIGAKU-DMAX2500 X-ray diffractometer using Cu-K α radiation ($\lambda = 1.542 \text{ \AA}$) with a scanning rate of 10° min⁻¹ and a step size of 0.02°. Thermalgravimetric analysis (TGA) was performed on a Perkin-Elmer TGA-7000 thermogravimetric analyzer with a heating rate of 10 °C min⁻¹. The solvent emulsion and solid fluorescent spectra of compound 4 were obtained on a HITACHI F-2700 fluorescence Spectrophotometer at room temperature.

3. Synthesis of compounds 1–4

3.1. Synthesis of [Cu(Hmthd)₂Cl]_n (1)

A solution of Hmthd (3.97 mg, 0.03 mmol) in ethanol (3 mL) was added to a solution of CuCl (1.98 mg, 0.02 mmol) in CH₃CN (3 mL), and the mixed solution was stirred for about 20 min. The pH value of the above mixture was adjusted through addition of 0.15 mL HCl (0.1 mol/L), then the mixture was sealed in a 20 mL Teflon-lined stainless-steel reactor

and heated at 80 °C for 72 h under autogenous pressure. After slowly cooling to room temperature, yellow rod-shaped crystals of 1 were collected by filtration and washed with distilled water and ethanol several times. Yield: 35% (based on the Hmthd). Elemental anal. calcd C₆H₈ClCuN₄S₄ (363.39): C, 19.81; H, 2.20; N, 15.41. Found: C, 19.85; H, 2.16; N, 15.44. IR data (KBr, cm⁻¹): 2904(w) 1479(w), 1419(w), 1335(s), 1188(m), 1079(m), 1025(m), 965(w), 768(m), 671(w), 622(w), 535(w).

3.2. Synthesis of [Cu₃(mthd)₂Br]_n (2)

The procedure was the same as that for compound 1 except that CuCl was replaced by CuBr (2.87 mg, 0.02 mmol). After slowly cooling to room temperature, yellow rhomboid crystals of 2 were collected by filtration and washed with distilled water and ethanol several times. Yield: 47% (based on the Hmthd). Elemental anal. calcd C₆H₈BrCu₃N₄S₄ (532.92): C, 13.51; H, 1.13; N, 10.51. Found: C, 13.55; H, 1.09; N, 10.55. IR data (KBr, cm⁻¹): 2909(w), 1566(w), 1452(m), 1349(s), 1108(s), 1039(w), 994(w), 884(w), 780(w), 617(vs).

3.3. Synthesis of [Ag(mthd)]_n (3)

A mixture of AgNO₃ (3.40 mg, 0.02 mmol), KBr (2.38 mg, 0.02 mmol) and Hmthd (2.64 mg, 0.02 mmol) was dissolved in a CH₃CH₂OH : CH₃CN solution (v : v = 3 : 2, 5 mL). The pH value of above mixture was adjusted through addition of 0.05 mL ethylenediamine (0.1 mol/L), then was sealed in a 20 mL Teflon-lined stainless-steel reactor and heated at 80 °C for 72 h under autogenous pressure. After slowly cooling to room temperature, white needle crystals of 3 were collected by filtration and washed with distilled water and ethanol several times. Yield: 43% (based on the Hmthd). Elemental anal. calcd C₃H₃AgN₂S₂ (239.06): C, 15.06; H, 1.25; N, 11.71. Found: C, 15.02; H, 1.19; N, 11.76. IR data (KBr, cm⁻¹): 2920(w), 1572(w), 1430(w), 1354(s), 1190(m), 1097(w), 1043(m), 977(w), 879(w), 769(m), 617(vs).

3.4. Synthesis of [Ag₂(mthd)]_n (4)

The procedure was the same as that for compound 3 except that KBr was replaced by KI (3.32 mg, 0.02 mmol). After slowly cooling to room temperature, white rhomboid crystals of 4 were collected by filtration and washed with distilled water and ethanol several times. Yield: 58% (based on the Hmthd). Elemental anal. calcd C₃H₃Ag₂IN₂S₂ (473.83): C, 7.60; H, 0.63; N, 5.91. Found: C, 7.58; H, 0.64; N, 5.93. IR data (KBr, cm⁻¹): 2920(w), 1474(w), 1414(w), 1363(vs), 1196(m), 1119(w), 1086(w), 1032(m), 972(w), 764(w), 737(w), 666(w), 617(w).

3.5. Single crystal structure determination

The crystal structures were determined by single-crystal X-ray diffraction. Reflection data were collected on a Bruker SMARTCCD area-detector diffractometer (Mo-K α radiation, graphite monochromator) at room temperature with ω -scan mode. Empirical adsorption correction was applied to all data using SADABS. The structure was solved by direct methods and refined by full-matrix least squares on F^2 using SHELXTL 2014 software [48]. Non-hydrogen atoms were refined anisotropically. All C-bound H atoms were refined using a riding model with Uiso(H) = 1.2. The crystallographic data and pertinent information are given in Table 1; the selected bond lengths and angles in Table S1.

4. Results and discussion

4.1. Synthesis of compounds 1–4

During the synthesis process, we found that ethanol is helpful to the dissolution of Hmthd ligand while MX (M = Ag^I or Cu^I, X = Cl⁻, Br⁻ or I⁻) can be soluble in acetonitrile, which provide a facility for solvothermal

Table 1
Crystal and structure refinement data for compounds 1–4.

Compound	1	2	3	4
Empirical formula	C ₆ H ₆ ClCuN ₄ S ₄	C ₆ H ₆ BrCu ₃ N ₄ S ₄	C ₃ H ₃ AgN ₂ S ₂	C ₃ H ₃ Ag ₂ IN ₂ S ₂
Formula weight	363.39	532.92	239.06	473.83
Crystal system	monoclinic	monoclinic	triclinic	orthorhombic
Space group	C2/c	P2 ₁ /n	P-1	Pca2 ₁
a/Å	15.922 (3)	8.650 (4)	4.1986 (2)	10.056 (4)
b/Å	5.9559 (8)	10.046 (4)	12.5171 (7)	11.206 (5)
c/Å	13.740 (2)	15.793 (6)	12.6172 (7)	7.964 (3)
α/°	90	90	64.4150 (10)	90
β/°	102.454 (9)	91.786 (15)	85.277 (2)	90
γ/°	90	90	86.921 (2)	90
Volume/(Å ³)	1272.3 (3)	1371.7 (10)	595.92 (6)	897.5 (7)
Z	4	4	4	4
ρ _{calc} /Mg/m ⁻³	1.897	2.581	2.665	3.507
Absorption coef.	2.559	8.112	3.960	8.196
Reflections collected	15,528	8293	11,951	8398
Unique (R _{int})	1446 (0.0213)	3083 (0.0711)	2073 (0.0288)	1909 (0.0516)
Completeness	99.4 %	97.9 %	96.9 %	94.0 %
Goof	1.102	1.038	1.210	1.119
R ₁ , wR ₂ [I > 2σ(I)] ^[a]	R ₁ = 0.0184, wR ₂ = 0.0467	R ₁ = 0.0683, wR ₂ = 0.1690	R ₁ = 0.0300, wR ₂ = 0.0822	R ₁ = 0.0308, wR ₂ = 0.0717
R ₁ , wR ₂ (all data) ^[a]	R ₁ = 0.0201, wR ₂ = 0.0482	R ₁ = 0.1389, wR ₂ = 0.2039	R ₁ = 0.0359, wR ₂ = 0.0850	R ₁ = 0.0347, wR ₂ = 0.0741

$$^{[a]}R_1 = \frac{\sum ||F_o| - |F_c||}{\sum |F_o|}; wR = \left[\frac{\sum w(F_o^2 - F_c^2)^2}{\sum w(F_o^2)^2} \right]^{1/2}.$$

reaction. As is well known, self-assembly processes under solvothermal conditions are often influenced by solvent composition, reaction temperature, solution pH, etc. The experiments show lower pH values (acidic conditions) are beneficial to the formation and growth of crystalline **1** and **2**, however, when alkaline substances such as ethylenediamine or NaOH as a regulator were added to the reaction system, some unrecognizable flocculent or powdery substances are often obtained. If CuCl and CuBr were replaced by CuI in acidic conditions, some unrecognizable fine solid powders were often obtained; When ethylenediamine adjusts the pH of the reaction system to alkaline conditions, (H₂en)SO₄ is easily obtained, and the possible reason is that Hmthd ligand is desulfurized and oxidized to SO₄²⁻. For compounds **3–4**, in acidic conditions, the crystals were too small to be characterized by single crystal X-ray diffraction, while weakly alkaline conditions are beneficial to the formation and growth of the targeted crystals suitable for characterization. Notably, it is difficult to get the target crystals of **3** through the reaction between AgNO₃ and Hmthd ligand. We have also tried to synthesize AgCl-based coordination complex, unfortunately, some small needle-like crystals were obtained but could not be characterized by single crystal X-ray diffraction. The successful synthesis of compounds **1–4** demonstrates that the composition of the solvent and the pH value of the solution played an important role in the preparation of Cu^I/Ag^I-based compounds containing Hmthd ligands.

5. Crystal structures of 1–4

5.1. Crystal structure of [Cu(Hmthd)₂Cl]_n (**1**)

Single-crystal X-ray diffraction shows that compound **1** crystallizes in the monoclinic system with space group C2/c. The asymmetric unit of compound **1** is composed of half a Cu(I) ion, half a chloride anion, one electrically neutral Hmthd ligand. Both Cu(I) and Cl⁻ are located on a 2₁ symmetry axis with occupancy of 0.5. The Cu(I) center shows a planar triangular geometry and coordinates with two sulfur atoms from two different neutral Hmthd ligand and one chloride ion (Fig. 1a). The Cu-S and Cu-Cl bond distances are 2.2211(5) and 2.2358(7) Å, respectively; and the S/Cl-Cu-S/Cl bond angles range from 118.737(13) to 122.52 (3)°. Notably, the C3-S2 bond length (1.69 Å) in neutral Hmthd ligand is apparently shorter than that of C-S bonds within aromatic 1,3,4-thiadiazole ring (d_{C2-S1} = 1.74 Å and d_{C3-S1} = 1.73 Å), indication C3-S2 bond has the characteristics of C=S double bond. Notably, all the

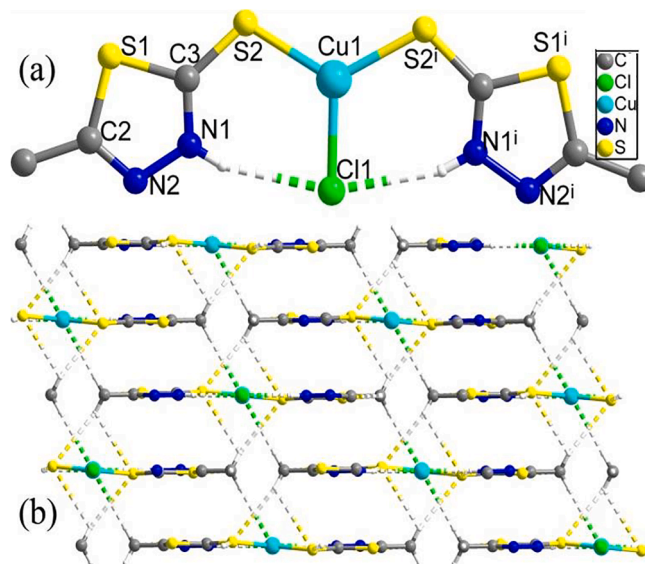


Fig. 1. (a) Coordination environment of the Cu(I) ion, (b) the 3D supramolecular network in compound **1**. The hydrogen atoms are omitted.

C-S bond distances observed in Hmthd ligand are longer than that of C=S double bond of 1.62 Å, while shorter than that of C-S single bond of 1.81 Å [24], indicating that partial C=S double bond characters in Hmthd ligand are observed. Therefore, the above results indicate there exist in a thione-thiol (-N=C-SH ↔ -NH-C=S) transformation equilibrium in Hmthd ligand.

Two neutral Hmthd molecules in a μ_{1-κ}2 coordination mode interact with one CuCl unit to form a mononuclear coordination compound, in which two neutral Hmthd molecules and CuCl unit are coplanar and the largest deviation is 0.1565 Å. The intra-molecular hydrogen bonds between protonated N1 and Cl⁻ anion play an important role in the formation of coplanar molecule. The coplanar mononuclear molecules are assembled into a three-dimensional (3D) supramolecular network through C-H...S and C-H...Cl hydrogen bonds (Fig. 1b).

5.2. Crystal structure of $[\text{Cu}_3(\text{mthd})_2\text{Br}]_n$ (2)

Single-crystal X-ray diffraction shows that compound **2** crystallizes in the monoclinic system with space group $P2_1/c$. The asymmetric unit of compound **2** is composed of three Cu(I) ions, two completely deprotonated (mthd)⁻ anions and one bromide anion. The Cu1 and Cu3 centers both display a distorted tetrahedral geometry, and Cu1 is bound to one sulfur atom and two nitrogen atoms from three different (mthd)⁻ anions and one bromide anion, while Cu3 is coordinated with two sulfur atoms, one nitrogen atom from three different (mthd)⁻ anions and one bromide anion. The Cu2 center exhibits a planar triangular geometry and is bound to two sulfur atoms and one nitrogen atom from three different (mthd)⁻ anions (Fig. 2a). The Cu–N, Cu–S and Cu–Br bond distances are in the range of 2.009(8)–2.040(9) Å, 2.258(3)–2.429(3) Å and 2.426(2)–2.460(3) Å, respectively, and the S/N/Br–Cu–S/N/Br bond angles range from 99.0(3) to 132.62(11)°. The C–S bond distances ($d_{\text{C}_4\text{S}_1} = 1.73$ Å and $d_{\text{C}_1\text{S}_3} = 1.74$ Å) outside the thiadiazole ring in compound **2** is equivalent to that inside the ring (average C–S bond length is 1.73 Å), but apparently longer than C–S bond distance (1.69 Å) in compound **1**. The (mthd)⁻ anion displays two kinds of coordination modes: $\mu_4-1\kappa\text{N}1$, $2\kappa\text{N}2$, $3\kappa\text{S}3$, $4\kappa\text{S}3$ and $\mu_5-1\kappa\text{N}3$, $2\kappa\text{N}4$, $3\kappa\text{S}1$, $4\kappa\text{S}1$, $5\kappa\text{S}1$ (Fig. 2b).

Two (mthd)⁻ anions containing S4 atom and two CuBr molecules coordinate with each other through Cu–N bonds to form an anionic $[\text{CuBr}(\text{mthd})]_2^{2-}$ unit with Cu...Cu distance of 3.44 Å (Fig. 2c), however, the (mthd)⁻ anion containing S2 atom links Cu2 and Cu3 ions into a 1D coplanar cationic $\{[\text{Cu}_2(\text{mthd})]^{+}\}_n$ chain with the shortest Cu...Cu distance of 3.33 Å through Cu–S and Cu–N bonds (Fig. 2d). The anionic $[\text{CuBr}(\text{mthd})]_2^{2-}$ units and 1D coplanar cationic $\{[\text{Cu}_2(\text{mthd})]^{+}\}_n$ chains are connected to each other to form a 2D layered structure through Cu–S, Cu–N and Cu–Br bonds (Fig. 2e).

5.3. Crystal structure of $[\text{Ag}(\text{mthd})]_n$ (3)

Single-crystal X-ray diffraction shows that compound **3** crystallizes in the triclinic system with space group $P-1$, its asymmetric unit contains two Ag⁺ ions and two completely deprotonated (mthd)⁻ anions. The Ag1 and Ag2 centers both display a distorted tetrahedral geometry, and Ag1 is bound to three sulfur atoms and one nitrogen atom from four different (mthd)⁻ anions, while Ag2 is coordinated with two sulfur atoms and two nitrogen atoms from four different (mthd)⁻ anions (Fig. 3a). The Ag–S

and Ag–N bond distances are in the range of 2.4593(19)–2.712(2) Å and 2.253(6)–2.630(6) Å, respectively, and the S/N–Ag–S/N bond angles range from 84.57(14) to 155.34(16)°. The C–S bond distances ($d_{\text{C}_1\text{S}_1} = 1.72$ Å and $d_{\text{C}_3\text{S}_4} = 1.71$ Å) outside the thiadiazole rings in compound **3** is slightly shorter than that inside thiadiazole ring (average C–S bond length is 1.74 Å), but slightly longer than C–S bond distance in compound **1**. The (mthd)⁻ anion displays two kinds of coordination modes: $\mu_4-1\kappa\text{N}1$, $2\kappa\text{S}1$, $3\kappa\text{S}1$, $4\kappa\text{S}1$ and $\mu_4-1\kappa\text{N}3$, $2\kappa\text{N}4$, $3\kappa\text{S}3$, $4\kappa\text{S}3$ (Fig. 3b).

The (mthd)⁻ anions containing S3 atoms interact with Ag1 ions through Ag–S and Ag–N bonds into a 1D puckered $[\text{Ag}(\text{mthd})]_n$ chain structure (marked as chain 1) in which two parallel zigzag (AgS) chains with the shortest Ag...Ag distance is 3.08 Å are observed (Fig. 3c), which is shorter than the sum of Vander Waals radius (3.44 Å) of Ag atoms, but slightly longer than that of the Ag–Ag separation in bulk metallic silver (2.89 Å) [49–50], indicating that obvious Ag–Ag interactions. Interestingly, similar 1D puckered $[\text{Ag}(\text{mthd})]_n$ chain (marked as chain 2) is formed through the interaction of (mthd)⁻ anions containing S1 atoms and Ag2 ions, and the corresponding shortest Ag...Ag distance is 3.11 Å (Fig. S1). Notably, two nitrogen atoms of thiadiazole ring in chain 1 are involved in the coordination with Ag ions, however, only one nitrogen atom of thiadiazole ring in chain 2 coordinates with Ag ions. The chains 1 and chains 2 are further connected to each other to form a 2D irregular layered structure through Ag–S and Ag–N bonds (Fig. 3d), in which a $(\text{AgS})_n$ chain constructed by staggered Ag_3S_3 rings is formed (Fig. 3e).

5.4. Crystal structure of $[\text{Ag}_2(\text{mthd})]_n$ (4)

Single-crystal X-ray diffraction shows that compound **4** crystallizes in the orthorhombic system with space group $Pca2_1$, its asymmetric unit is composed of two Ag⁺ ions, one completely deprotonated (mthd)⁻ anion and one I⁻ anion. The Ag1 and Ag2 centers both display distorted tetrahedral geometries, and Ag1 is bound to two sulfur atoms and one nitrogen atom from three different (mthd)⁻ anions and one I⁻ anion, while Ag2 is coordinated with one sulfur atom and one nitrogen atom from two different (mthd)⁻ anions and two I⁻ anions (Fig. 4a). The Ag–S and Ag–N bond distances are in the range of 2.528(3)–2.893(3) Å and 2.290(8)–2.421(10) Å, respectively, and the S/N–Ag–S/N bond angles range from 93.33(5) to 116.4(2)°. The C–S bond distances ($d_{\text{C}_3\text{S}_2} = 1.73$ Å) outside the thiadiazole rings in compound **4** is equivalent to that inside the ring (average C–S bond length is 1.73 Å), similar to the

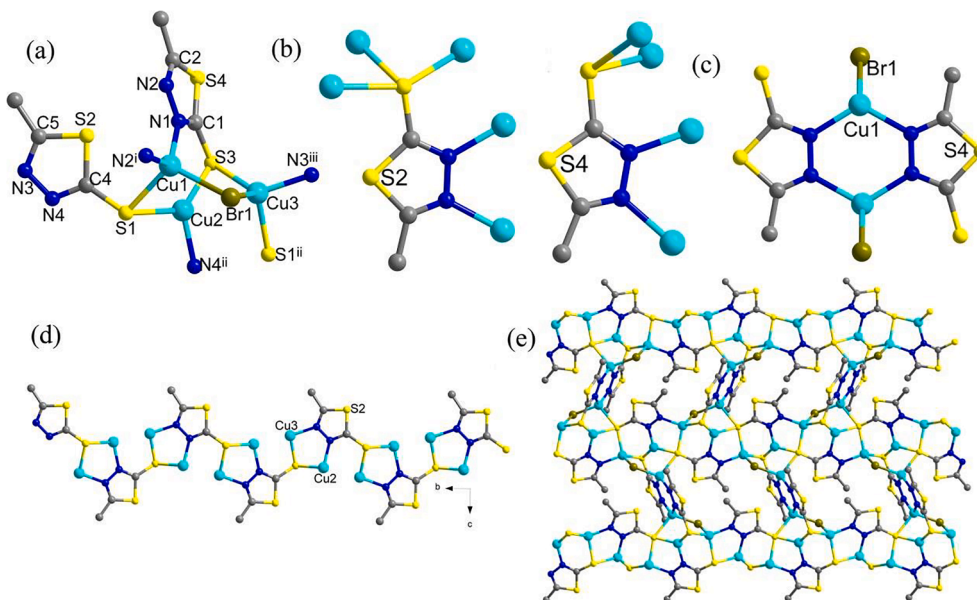


Fig. 2. (a) Coordination environments of the Cu(I) ions, (b) coordination modes of (mthd)⁻ anion, (c) $[\text{CuBr}(\text{mthd})]_2^{2-}$ unit, (d) 1D coplanar cationic $\{[\text{Cu}_2(\text{mthd})]^{+}\}_n$ chain, (e) the 2D layer in compound **2**. The hydrogen atoms are omitted.

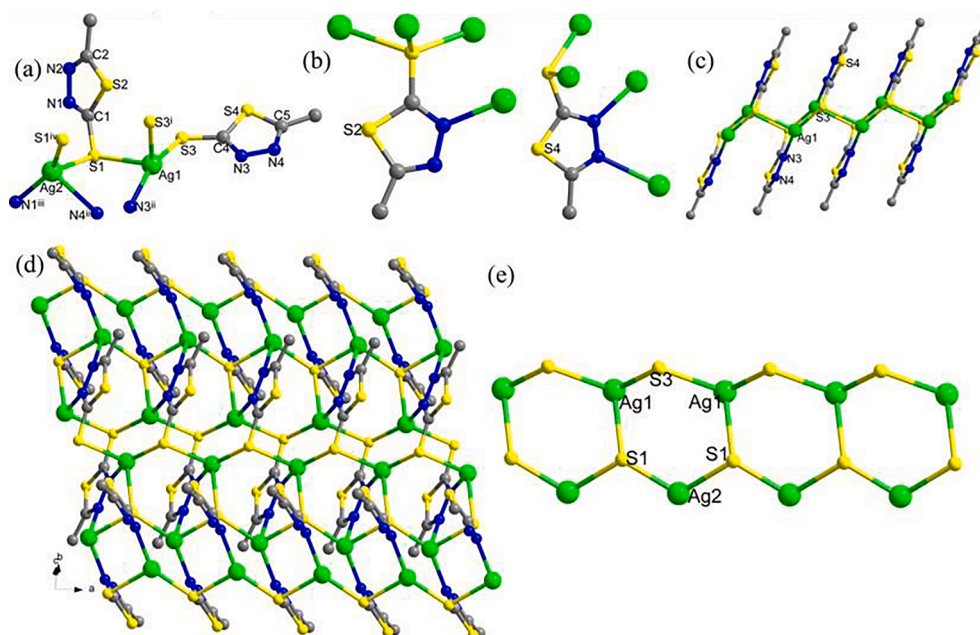


Fig. 3. (a) Coordination environments of the Ag(I) ions, (b) coordination modes of (mthd)⁻ anion, (c) 1D puckered [Ag(mthd)]_n chain (Chain 1), (d) 2D irregular layered structure, (e) the (AgS)_n chain constructed by staggered Ag₃S₃ rings in compound 3. The hydrogen atoms are omitted.

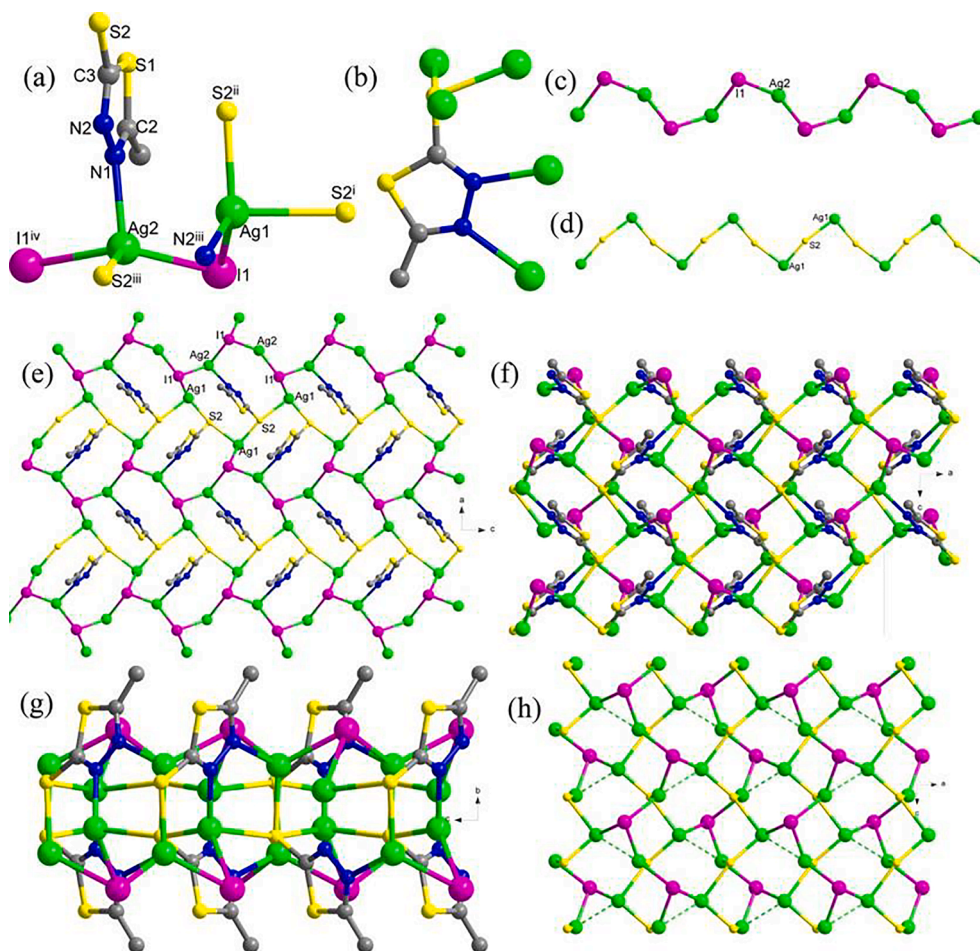


Fig. 4. (a) Coordination environments of the Ag(I) ions, (b) coordination mode of (mthd)⁻ anion, (c) 1D inorganic (AgI)_n chain, (d) 1D zigzag inorganic (AgS)_n chain, (e) 2D organic-inorganic layer, (f) 2D double-layer structure along *ac* plane, (g) 2D double layer structure along *bc* plane, (h) 2D inorganic (Ag₂IS)_n double layer in compound 4. The hydrogen atoms are omitted.

(mthd)⁻ anion in compound **2**. Each (mthd)⁻ anion coordinates with five Ag(I) ions through μ_5 -1 κ N1, 2 κ N2, 3 κ S2, 4 κ S2, 5 κ S2 coordination mode (Fig. 4b), and each I⁻ anion joins three Ag(I) ions in a μ_3 coordination mode. Interestingly, the three silver ions connected to the sulfur atom of the (mthd)⁻ anion in compound **4** are evenly arranged in a semicircle and the corresponding Ag-S-Ag bond angles range from 79.46° to 163.48°, however, the three silver ions bound to the sulfur atom of the (mthd)⁻ anion containing S2 atom in compound **3** are evenly arranged in a circle and the corresponding Ag-S-Ag bond range from 99.47° to 120.46°.

The I⁻ anions link Ag₂ ions to form an 1D inorganic (AgI)_n chain with the shortest Ag...Ag distance of 4.16 Å (Fig. 4c), and the S2 atoms of (mthd)⁻ anions and Ag1 ions are connected to each other to assemble a 1D zigzag inorganic (AgS)_n chain with the shortest Ag...Ag distance of 5.42 Å (Fig. 4d). Then the (AgI)_n and (AgS)_n chains are further assembled into a 2D inorganic (Ag₂IS)_n layer through Ag-I bonds with the shortest Ag...Ag distance of 3.15 Å, in which a 10-membered ring constructed by two S ions, three I⁻ anions and five Ag⁺ ions is observed. Notably, thiazazole rings of (mthd)⁻ anions located in the 10-membered rings link (AgI)_n and (AgS)_n chains through Ag-N and C-S bonds to form a 2D organic-inorganic layer (Fig. 4e). The 2D organic-inorganic layers are further joined into a 2D double layer through Ag-S bonds (Fig. 4f and Fig. 4g), interestingly, a 2D inorganic (Ag₂IS)_n double layer is formed (Fig. 4h), where the interactions between the organic ligands and the inorganic layers are conducive to the stability of the 2D layer.

5.5. Characterization

The PXRD patterns of compounds **1–4** are consistent with the simulated patterns generated by single crystal X-ray diffraction data (Fig. S2), indicating the high purity of the obtained crystalline products of compounds **1–4**, and the different intensities between the simulated and experimental patterns may be attributed to the preferred orientation of the powder samples.

Fig. S3 shows the FT-IR spectra of compounds **1–4** and Hmthd. Notably, the wide absorption peaks located at 3050 cm⁻¹ and 2867 cm⁻¹ can be ascribed to the stretching vibration of the N-H and S-H bonds in the IR spectrum of Hmthd ligand [46], respectively, however, the adsorption peaks in this region for compounds **1–4** disappeared, possibly due to the deprotonation of N-H and S-H bonds or thionethiol (-N=C-SH ↔ -NH-C=S) tautomeric transformation. The characteristic peaks at 1456 cm⁻¹ and 1384 cm⁻¹ correspond to the symmetric and asymmetric stretching vibrations of the C=N and C=C bonds [37], respectively. Notably, the absorption peaks of N-N bonds of (mthd)⁻ might appear to overlap significantly with that of C=N and C=C bonds. The multiple peaks ranging from 1260 cm⁻¹ to 1039 cm⁻¹ in the IR spectrum of Hmthd ligand are related to the C-S bond, while the disappearance of the peak at 1260 cm⁻¹ in compounds **1–4** may be due to the coordination of S with metal ions [51–52].

To investigate thermal stability of compounds **1–4**, their thermal-gravimetric analyses (TGA) were measured under nitrogen atmosphere from 30 °C to 800 °C, and the corresponding TGA curves shown in Fig. S4 have similar thermal behaviors with a one-step loss weight. The frameworks of compounds **1–4** were thermally stable up to 272 °C, further heating, due to the decomposition of the organic linkers, the skeletons began to collapse rapidly.

5.6. Luminescence property

The fluorescence of compounds **1–3** and Hmthd ligand are too weak to be observed under ultraviolet light and difficult to be detected on a fluorescence spectrometer, however, compound **4** gives off apparent yellow light under the ultraviolet lamp, perhaps due to the combined effect of short Ag...Ag interactions, Ag₃I cluster, molecular packing, and so on [14,53]. The solid-state fluorescence spectrum of compound **4** at room temperature exhibits yellow light emission with the maximum at 551 nm when excited at 333 nm (Fig. 5).

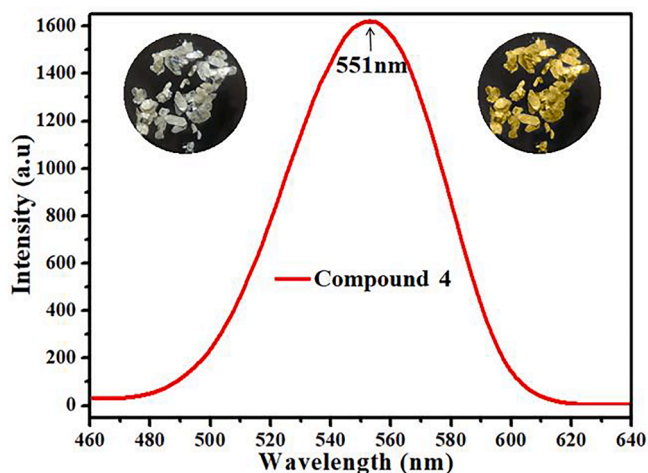


Fig. 5. Solid-state emission spectrum of compound **4**. Insets are the photo images of compound **4** under daylight (left) and UV illumination (right) at 365 nm, respectively.

In order to investigate the potential application of **4** for small molecule sensing, 4-solvent emulsions were prepared by immersing 1.0 mg ground crystals of **4** into 2.00 mL of acetonitrile, dichloromethane (CH₂Cl₂), dimethylacetamide (DMA), N,N-dimethyl-formamide (DMF), ethanol, ethylene glycol, H₂O, methanol, formaldehyde, and NB, and then the corresponding PL spectra were measured after 4-solvent emulsions are dispersed by ultrasound for about 5 min. Fig. 6a shows the peak shapes and peak positions of emission spectra of 4-solvent emulsions ($\lambda_{\text{ex}} = 333$ nm) are similar to that of solid-state fluorescence spectrum of compound **4**, while the fluorescent intensities vary with the solvent molecules. The maximum luminescence intensity of 4-solvent emulsions gradually decreased in the following order: ethanol > H₂O > CH₂Cl₂ > acetonitrile > methanol > formaldehyde > ethylene glycol > DMA > DMF > NB. Obviously, 4-ethanol emulsion shows the strongest fluorescence, however, the fluorescence of 4-NB emulsion can't be detected, indicating that NB is an effective quencher and results in a nearly 100% fluorescence quenching for compound **4**. All 4-solvent emulsions under UV light except NB showed obvious yellow light emission (Fig. 6b), such solvent-dependent luminescence quenching might become an effective luminescent sensing probe for NB molecules.

Fluorescence-quenching titration tests were performed with an incremental addition of NB (0.01 mol/L) to 4-ethanol emulsion as a standard emulsion. Fig. 6c shows that the fluorescence intensity of the 4-ethanol emulsion gradually decreased with increasing NB concentration, when the concentration of NB increased to 0.225 mM, 93% fluorescence intensity was quenched. The fluorescence quenching efficiency was further analyzed using the Stern-Volmer (SV) equation: $I_0/I = 1 + K_{\text{SV}} [M]$ (where I_0 is the initial fluorescence intensity of the 4-ethanol emulsion without NB molecules, I is the fluorescence intensity of 4-ethanol emulsion with NB molecules, K_{SV} is the quenching constant (M⁻¹), $[M]$ is the molar concentration of NB). The SV plot for NB was nearly linear at low concentrations and subsequently deviated from linearity, bending upwards at higher concentrations (Fig. 6d). The K_{SV} value of compound **4** for NB is 5.07×10^3 M⁻¹, higher than that of the reported fluorescent MOF sensors for the detection of NB in the organic phase (Table 2), indicating a higher quenching efficiency. According to 3 σ /K equation (where σ is the standard deviation and K is the slope of the fitting curve of the luminescence intensity of **4** at different analyte concentration), the detection limit of NB is 5.33×10^{-6} M. The above-mentioned result revealed that compound **4** could be a promising luminescent probe for sensing NB molecules. Additionally, the recyclable performance of **4** for NB sensing were also investigated and found that compound **4** can be easily regenerated by washing with distilled ethanol after five runs tests (Fig. S5).

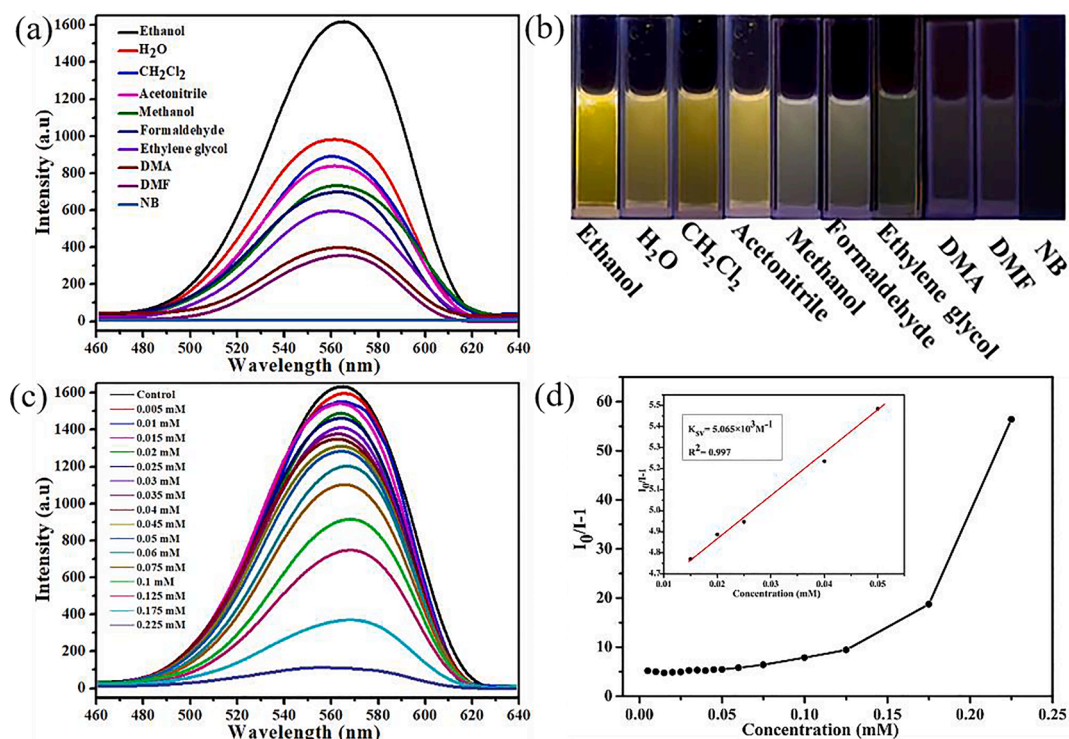


Fig. 6. (a) Emission spectra of compound 4 in different solvents when excited at 333 nm, (b) luminescence photographs of compound 4 in different solvent emulsions under UV light, (c) the fluorescence titration of 4-ethanol emulsion with the addition of different concentrations of NB, (d) the Stern-Volmer plot for the luminescence intensity of 4 upon addition of NB solution in ethanol. The insert is Stern-Volmer plot at low analytes concentrations.

Table 2

Comparison among various MOF-based sensors for detection of NB.

MOFs	dispersion solvent	K _{SV} [M ⁻¹]	Refs.
[Zn ₃ (TTPA) ₂ (DHTP) ₃]-2DMF	ethanol	1.86 × 10 ²	[54]
[Zn(L)(dipb)]·(H ₂ O) ₂	DMA	2.31 × 10 ²	[55]
[Zn ₂ (L) ₂ (dpyb)]	DMA	3.09 × 10 ²	[55]
{[Tb ₂ (L) ₃ (H ₂ O) ₄ ·10H ₂ O] _n }	DMF	1.8 × 10 ³	[56]
{[Cd ₂ (L)(DMA)]·[H ₂ N(Me) ₂] _n }	DMA	2.7 × 10 ³	[57]
{[Zn(L)](DMF) ₃] _n }	methanol	2.87 × 10 ³	[58]
[Zn ₂ (NDC) ₂ (bpy)]·G _x	ethanol	3.05 × 10 ³	[59]
Zn ₃ (BTC) ₂ : 4% Eu(III)	methanol	3.95 × 10 ³	[60]
[(Pr ₂ (TATMA) ₂)-4DMF·4H ₂ O] _n	DMF	4.1 × 10 ³	[61]
[Ag ₂ (mthd)] _n	ethanol	5.07 × 10 ³	This work

To analyze the mechanism of luminescent quenching by NB, the IR spectrum and PXRD pattern of 4 after immersion in NB were measured. The IR spectrum and PXRD pattern of compound 4 after immersion in NB matched well with that obtained from the untreated crystals of compound 4 (Fig. S3 and Fig. S6), indicating that the framework of 4 can be kept intact in NB. Therefore, the fluorescence quenching behavior was not caused by the framework collapse. In order to further investigate the quenching mechanism, the UV-Vis spectra of NB and other solvents were measured (Fig. S7). The results reveal that only NB have a strong absorption ranging from 300 to 440 nm, while other solvents have no significant absorption in this range. Notably, the excitation wavelength of the compound 4 is 333 nm, which is completely overlapped by the absorbing band of NB. So, the efficient quenching of NB in this system might be ascribed to a competition for the excitation energy between the emission band of the fluorophore and the absorption band of the analyte [25,27,62]. Moreover, the luminescence quenching behavior may be due to the electron transfer from the electron-donating materials to the electron-deficient NB molecules [55,63–64].

6. Conclusion

In summary, four new coordination compounds based on Hmthd ligand have been synthesized and characterized in detail. Compounds 1–4 display rich structural chemistry ranging from 0 D (1) to 2 D (2–4) structures, providing a new strategy to construct the Cu^I/Ag^I-based coordination compounds containing Hmthd ligands with extended structures through the synergistic effect of (mthd)⁻ and halide ions. Notably, compound 4 shows efficiently fluorescent quenching response to NB molecules. The further research for the construction of new fluorescent coordination compounds based on organic sulfur ligands is underway in our laboratory.

CRedit authorship contribution statement

Ying Geng: Methodology, Software, Writing - original draft. **Wen Zhang:** Validation, Investigation, Writing - original draft. **Jiang-Feng Song:** Conceptualization, Formal analysis, Resources, Supervision, Writing - review & editing, Project administration. **Rui-Sha Zhou:** Writing - review & editing. **Wei-Zhou Jiao:** Project administration.

Declaration of Competing Interest

The authors declare that they have no known competing financial interests or personal relationships that could have appeared to influence the work reported in this paper.

Acknowledgements

This work was supported by the National Natural Science Foundation of China (No.: 21961027), the Natural Science Foundation of Shanxi Province (No.: 201801D121068), the Foundation of Shanxi Province Key Laboratory of Hige Oriented Chemical Engineering (No. CZL2020-05), Foundation of State Key Laboratory of High-efficiency Utilization of

Coal and Green Chemical Engineering (Grant No. 2019-KF-25), respectively.

Appendix A. Supplementary data

CCDC numbers 2095361–2095364 contain the supplementary crystallographic data for compounds 1–4. These data can be obtained free of charge via <http://www.ccdc.cam.ac.uk/conts/retrieving.html>, or from the Cambridge Crystallographic Data Centre, 12 Union Road, Cambridge CB2 1EZ, UK; fax: (+44) 1223-336-033; or e-mail: deposit@ccdc.cam.ac.uk. Supplementary data associated with this article: the PXRD, TGA, UV spectra, IR spectra and Table S1 for compounds 1–4 can be found online. Supplementary data to this article can be found online at <http://doi.org/10.1016/j.ica.2021.120596>.

References

- M.D. Allendorf, C.A. Bauer, R.K. Bhakta, R.J.T. Houk, Luminescent metal-organic frameworks, *Chem. Soc. Rev.* 38 (5) (2009) 1330, <https://doi.org/10.1039/b802352m>.
- O.V. Dolomanov, A.J. Blake, N.R. Champness, M. Schröder, C. Wilson, A novel synthetic strategy for hexanuclear supramolecular architectures, *Chem. Commun.* 6 (2003) 682–683.
- M.K. Bera, L. Behera, S. Mohapatra, A fluorescence turn-down-up detection of Cu²⁺ and pesticide quinalphos using carbon quantum dot integrated UiO-66-NH₂, *Colloid. Surface. A.* 624 (2021), 126792.
- F.W. Steuber, J.J. Gough, É. Whelan, L. Burtynak, A.L. Bradley, W. Schmitt, Node-Dependent Photoinduced Electron Transfer in Third Generation 2D MOFs Containing Earth- Abundant Metal Ions, *Inorg. Chem.* 59 (23) (2020) 17244–17250.
- M. Fumanal, C. Corminboeuf, B. Smit, I. Tavernelli, Optical absorption properties of metal-organic frameworks: solid state versus molecular perspective, *Phys. Chem.* 22 (35) (2020) 19512–19521.
- G.Z. Chen, W.S. Bai, Y. Jin, J.B. Zheng, Fluorescence and electrochemical assay for bimodal detection of lead ions based on Metal-Organic framework nanosheets, *Talanta* 232 (2021), 122405.
- Z.P. Zhang, Y. Liu, P.C. Huang, F.Y. Wu, L.H. Ma, Polydopamine molecularly imprinted polymer coated on a biomimetic iron-based metal-organic framework for highly selective fluorescence detection of metronidazole, *Talanta* 232 (2021), 122411.
- C.Y. Yue, B. Hu, X.W. Lei, R.Q. Li, F.Q. Mi, H. Gao, Y. Li, F. Wu, C.L. Wang, Novel Three Dimensional Semiconducting Materials Based on Hybrid d¹⁰ Transition Metal Halogenides as Visible Light-Driven Photocatalysts, *Inorg. Chem.* 56 (2017) 10962–10970.
- A. Hazra, S. Bej, A. Mondal, N.C. Murmu, P. Banerjee, Discerning Detection of Mutagenic Biopollutant TNP from Water and Soil Samples with Transition Metal-Containing Luminescence Metal-Organic Frameworks, *ACS. Omega.* 5 (2020) 15949–15961.
- Q. Li, D.X. Xue, Y.F. Zhang, Z.H. Zhang, Z.W. Gao, Syntheses, crystal structures and photoluminescence properties of five Cd/Zn-organic frameworks, *J. Mol. Struct.* 1164 (2018) 123–128.
- Y.-X. Ma, Y.-P. Gong, C.-I. Hu, J.-G. Mao, F. Kong, Three New d¹⁰ transition metal selenites containing PO₄ tetrahedron: Cd₇(HPO₄)₂(PO₄)₂(SeO₃)₂, Cd₆(PO₄)_{1.34}(SeO₃)_{4.66} and Zn₃(HPO₄)₂(SeO₃)₂(H₂O), *J. Solid. State. Chem.* 262 (2018) 320–326.
- C.L. Chen, B.S. Kang, C.Y. Su, Recent advances in supramolecular design and assembly of silver(I) coordination polymers, *Aust. J. Chem.* 59 (2006) 3–18.
- P.J. Steel, C.M. Fitchett, Metallo- supramolecular silver(I) assemblies based on pyrazine and related ligands, *Coord. Chem. Rev.* 252 (2008) 990–1006.
- X.W. Lei, F.X. Zhou, M.F. Wang, H.P. Zhang, C.Y. Yue, M.C. Hong, Synthesis, crystal structure and characterization of new tetranuclear Ag(I) complex with 5-aminoisophthalate, *Inorg. Chem.* 27 (2013) 171–174.
- K.Y. Yi, L. Zhang, Designed Eu(III)-functionalized nanoscale MOF probe based on fluorescence resonance energy transfer for the reversible sensing of trace Malachite green, *Food. Chem.* 354 (2021), 129584.
- X.L. Jin, G.T. Xu, Z.N. Chen, Recent advances in lanthanide luminescence with metal-organic chromophores as sensitizers, *Coord. Chem. Rev.* 273 (2014) 47–62.
- D.L. Shi, X.P. Yang, H.F. Chen, D.M. Jiang, J.N. Liu, Y.N. Ma, D. Schipper, R. A. Jones, Large Ln(42) coordination nanorings: NIR luminescence sensing of metal ions and nitro explosives, *Chem. Commun.* 55 (2019) 13116–13119.
- J.Q. Lin, C. Xiong, J.H. Xin, M. Li, W.H. Guo, F. Liu, X.L. Tong, Y.C. Ge, Structural variation and luminescence properties of d(10) metal ions complexes from 5-Aminotriazole ligand, *J. Mol. Struct.* 1166 (2018) 1–6.
- X. Feng, L. Liu, J.G. Zhou, L.L. Zhou, Z.Q. Shi, L.Y. Wang, A New Zn (II) Coordination Polymer Based on 4-(1-H-imidazol-2-yl) Benzoic Acid Ligand: Synthesis, Crystal Structure, and Photoluminescence Property, *Synth. React. Inorg. M.* 43 (6) (2013) 705–709.
- M. Stollenz, Linear Copper Complex Arrays as Versatile Molecular Strings: Syntheses, Structures, Luminescence, and Magnetism, *Chem. Eur. J.* 25 (2019) 4274–4298.
- G.F. Manbeck, W.W. Brennessel, R. Eisenberg, Photoluminescent Copper(I) Complexes with Amido- Triazolato Ligands, *Inorg. Chem.* 50 (8) (2011) 3431–3441.
- M. Wallech, D. Volz, D.M. Zink, U. Schepers, M. Nieger, T. Baumann, S. Bräse, Bright Coppertunities: Multinuclear CuI Complexes with N-P Ligands and Their Applications, *Chem. Eur. J.* 20 (22) (2014) 6578–6590.
- V.A. Krylova, P.I. Djurovich, B.L. Conley, R. Haiges, M.T. Whited, T.J. Williams, M. E. Thompson, Control of emission colour with N-heterocyclic carbene (NHC) ligands in phosphorescent three-coordinate Cu(I) complexes, *Chem. Commun.* 50 (2014) 7176–7179.
- Y.L. Wang, N. Zhang, Q.Y. Liu, Z.M. Shan, R. Cao, M.S. Wang, J.J. Luo, E.L. Yang, Diversity of architecture of copper(I) coordination polymers constructed of copper (I) halides and 4-Methyl-1,2,4-Triazole-3-Thiol (Hmptrz) Ligand: Syntheses, Structures, and Luminescent Properties, *Cryst. Growth. Des.* 11 (1) (2011) 130–138.
- R.S. Zhou, Z.Z. Lin, L.D. Xin, J.F. Song, H. Liu, Z.H. Guo, Naked eye colorimetric multifunctional sensing of nitrobenzene, Cr(VI) and Fe(III) with a new green emission Ag₆S₆ multi-metal-cluster, *Adv Compos. Mater.* 1 (4) (2018) 785–796.
- D. Urankar, B. Pinter, A. Pevec, F.D. Proft, I. Turel, J. Kosmrj, Click-Triazole N₂ Coordination to Transition-Metal Ions Is Assisted by a Pendant Pyridine Substituent, *Inorg. Chem.* 49 (2010) 4820–4829.
- J.F. Song, Y. Li, R.S. Zhou, T.P. Hu, Y.L. Wen, J. Shao, X.B. Cui, A novel 3D Cu(I) coordination polymer based on Cu₆Br₂ and Cu₂(CN)₂ SBUs: in situ ligand formation and use as a naked-eye colorimetric sensor for NB and 2-NT, *Dalton Trans.* 45 (2016) 545–551.
- J.F. Song, J. Wang, S.Z. Li, Y. Li, R.S. Zhou, Five new complexes based on 1-phenyl-1H-tetrazole-5-thiol: Synthesis, structural characterization and properties, *J. Mol. Struct.*, 1129 (2017) 1–7.
- J.F. Song, S.Z. Li, R.S. Zhou, J. Shao, X.M. Qiu, Y.Y. Jia, J. Wang, X. Zhang, Three novel Cu₆S₆ cluster- based coordination compounds: synthesis, framework modulation and the sensing of small molecules and Fe³⁺ ions, *Dalton Trans.* 45 (2016) 11883–11891.
- C.-W. Hsu, C.-C. Lin, M.-W. Chung, Y. Chi, G.-H. Lee, P.-T. Chou, C.-H. Chang, P.-Y. Chen, Systematic Investigation of the Metal-Structure-Photophysics Relationship of Emissive d¹⁰-Complexes of Group 11 Elements: The Prospect of Application in Organic Light Emitting Devices, *J. Am. Chem. Soc.* 133 (31) (2011) 12085–12099.
- R.-S. Zhou, W. Zhang, L.-D. Xin, H.-F. Wen, X.-Y. Zhang, L.-J. Su, J.-F. Song, A novel binary Cu₂I₂ and Cu₆S₆ cluster-based red emission compound and sensing of Cr(VI) in water, *Inorg. Chem. Commun.* 98 (2018) 154–158.
- X.C. Shan, F.L. Jiang, D.Q. Yuan, H.B. Zhang, M.Y. Wu, L. Chen, J. Wei, S.Q. Zhang, J. Pan, M.C. Hong, A multi-metal-cluster MOF with Cu₄I₄ and Cu₆S₆ as functional groups exhibiting dual emission with both thermochromic and near-IR character, *Chem. Sci.* 4 (2013) 1484–1489.
- S. Hu, F.-Y. Yu, P. Zhang, D.-R. Lin, In situ amination and side group effect of multifunctional heterocyclic thione ligand toward discrete and polymeric cluster constructions, *Dalton Trans.* 42 (21) (2013) 7731, <https://doi.org/10.1039/c3dt50165e>.
- S. Sun, L.-J. Liu, W.-Y. Ma, W.-X. Zhou, J. Li, F.-X. Zhang, Three complexes of Cu(I) cluster with flexible and rigid ligands: Synthesis, characterization and photoluminescent properties, *J. Solid. State. Chem.* 225 (2015) 1–7.
- Y. Han, H. Zheng, K. Liu, H. Wang, H. Huang, L.-H. Xie, L. Wang, J.-R. Li, In-Situ Ligand Formation- Driven Preparation of a Heterometallic Metal-Organic Framework for Highly Selective Separation of Light Hydrocarbons and Efficient Mercury Adsorption, *ACS. Appl. Mater. Inter.* 8 (35) (2016) 23331–23337.
- A.K. Jana, S. Natarajan, Cu₆S₆ Clusters as a Building Block for the Stabilization of Coordination Polymers with NiAs, NaCl, and Related Structures: Synthesis, Structure, and Catalytic Studies, *Eur. J. Inorg. Chem.* 6 (2018) 739–750.
- X.-Q. Liang, R.K. Gupta, Y.-W. Li, H.-Y. Ma, L.-N. Gao, C.-H. Tung, D.i. Sun, Structural Diversity of Copper(I) Cluster-Based Coordination Polymers with Pyrazine-2-thiol Ligand, *Inorg. Chem.* 59 (5) (2020) 2680–2688.
- I. Tsyba, B.B. Mui, R. Bau, R. Noguchi, K. Nomiyama, Synthesis and Structure of a Water-Soluble Hexanuclear Silver(I) Nicotinate Cluster Comprised of a “Cyclohexane-Chair”-Type of Framework, Showing Effective Antibacterial and Antifungal Activities: Use of “Sparse Matrix” Techniques for Growing Crystals of Water-Soluble Inorganic Complexes, *Inorg. Chem.* 42 (2003) 8028–8032.
- A.A. Ibrahim, H. Khaledi, H.M. Ali, A multiprotic indole-based thiocarbonylhydrazone in the formation of mono-, di- and hexa-nuclear metal complexes, *Polyhedron.* 81 (2014) 457–464.
- Z. Wang, R. Senanayake, C.M. Aikens, W.-M. Chen, C.-H. Tung, D.i. Sun, Gold-doped silver nanocluster [Au₃Ag₃₈(SCH₂Ph)₂₄X₅]²⁻ (X = Cl or Br), *Nanoscale.* 8 (45) (2016) 18905–18911.
- J. Han, Y. Liu, J. Lu, C. Tang, F. Wang, Y. Shen, Y. Zhang, D. Jia, Heterometallic sulfide cluster [Ag₆Sn₆S₂₀]¹⁰⁻: Solvothermal syntheses and characterizations of silver thioannates with lanthanide complex counter cations, *Inorg. Chem. Commun.* 57 (2015) 18–21.
- Z. Chen, L. Zhang, F. Liu, R. Wang, D. Sun, Anion-controlled formation of two silver lamella frameworks based on in situ ligand reaction, *CrystEngComm.* 15 (44) (2013) 8877, <https://doi.org/10.1039/c3ce40809d>.
- H.-B. Zhu, S.-H. Gou, In situ construction of metal-organic sulfur-containing heterocycle frameworks, *Coord. Chem. Rev.* 255 (1–2) (2011) 318–338.
- J.-F. Song, Y.-Y. Jia, J. Shao, R.-S. Zhou, S.-Z. Li, X. Zhang, Three new complexes based on methylpyrimidine-2-thione: in situ transformation, crystal structures and properties, *J. Coord. Chem.* 69 (20) (2016) 3072–3083.
- P. Bharati, A. Bharti, M.K. Bharti, S. Kashyap, U.P. Singh, N.K. Singh, Synthesis, spectral and structural characterization of Ni(II), Cu(II), Zn(II), Cd(II) and Hg(II) complexes with 2- mercapto- 5-methyl-1,3,4- thiadiazole: A Zn(II) complex acting

- as a new sensitive and selective fluorescent probe for the detection of Hg^{2+} in H_2O -MeOH medium, *Polyhedron*. 31 (2013) 222–231.
- [46] P. Bharati, A. Bharti, P. Nath, S. Kumari, N.K. Singh, M.K. Bharty, Square planar Pd(II) complexes derived from 1-ethyl-3-phenylthiourea, 3-mercapto-4-methyl-1,2,4-triazole and 2-mercapto-5-methyl-1,3,4-thiadiazole: Syntheses, spectral, structural characterization and photo-luminescence properties, *Inorg. Chem. Acta*. 443 (2016) 160–169.
- [47] C.L. Ma, J.K. Li, R.F. Zhang, Syntheses, Characterizations, and Crystal Structures of Tri- and Diorganotin(IV) Derivatives with 2-Mercapto-5-methyl-1,3,4-thiadiazole, *Heteroatom. Chem.* 17 (2006) 353–364.
- [48] G.M. Sheldrick, Crystal structure refinement with SHELXL, *Acta Crystallogr. Sect. C: Struct. Chem.* 71 (2015) 3–8.
- [49] W. Han, L. Yi, Z.Q. Liu, W. Gu, S.P. Yan, P. Cheng, D.Z. Liao, Z.H. Jiang, Synthesis and Characterisation of Two Supramolecular Polymers $[\text{CuAg}_4(\text{CN})_6(\text{tacn})]_n$ and $[\text{CuAu}_2(\text{CN})_4(\text{tacn})]_n$ Containing Metal Interactions, *Eur. J. Inorg. Chem.* 10 (2004) 2130–2136.
- [50] A.H. Chen, S.C. Meng, J.F. Zhang, C. Zhang, Two interesting tetranuclear Ag(I) complexes based on dipyrrodo [3,2-f:2,3-h]-quinoxaline: Synthesis, structural, luminescence and theoretical studies, *Inorg. Chem. Commun.* 35 (2013) 276–280.
- [51] M.K. Bharty, R.K. Dani, S.K. Kushawaha, N.K. Singh, R.N. Kharwar, R.J. Butcher, Mn(II), Ni(II), Cu(II), Zn(II), Cd(II), Hg(II) and Co(II) complexes of 1-phenyl-1H-tetrazole-5-thiol: Synthesis, spectral, structural, characterization and thermal studies, *Polyhedron*. 88 (2015) 208–221.
- [52] R.S. Zhou, X.Y. Zhang, J. Fu, L.D. Xin, W.Z. Jiao, J.F. Song, Four new Cu₆S₆ cluster-based coordination compounds: synthesis, crystal structures and fluorescence properties, *Dalton Trans.*, 50 (2021) 4567–4576.
- [53] J.Z. Huo, X.M. Su, X.X. Wu, Y.Y. Liu, B. Ding, Hydrothermal synthesis and characterization of a series of luminescent Ag(I) coordination polymers with two new multidentate bis-(1,2,3-triazole) ligands: structural diversity, polymorphism and photoluminescent sensing, *CrystEngComm*. 18 (2016) 6640–6652.
- [54] C.M. Ngue, M.K. Leung, K.L. Lu, An Electroactive Zinc-based Metal-Organic Framework: Bifunctional Fluorescent Quenching Behavior and Direct Observation of Nitrobenzene, *Inorg. Chem.* 59 (2020) 2997–3003.
- [55] Z.Q. Shi, Z.J. Guo, H.G. Zheng, Two Luminescent Zn(II) Meta-Organic Frameworks For Exceptionally Selective Detection of picric acid explosive, *Chem. Commun.* 51 (2015) 8300–8303.
- [56] Z. Sun, P. Hu, Y. Ma, L.C. Li, Lanthanide organic frameworks for luminescence sensing of nitrobenzene and nitrophenol with high selectivity, *Dyes Pigm.* 143 (2017) 10–17.
- [57] Y.T. Yan, J. Liu, G.P. Yang, F. Zhang, Y.K. Fan, W.Y. Zhang, Y.Y. Wang, Highly selective luminescence sensing for the detection of nitrobenzene and Fe^{3+} by new Cd(II)-based MOFs, *CrystEngComm*. 20 (2018) 477–486.
- [58] L. Wei, J. Lou, L. Liu, X.Z. Ma, J. Li, R. Pan, Y.X. Zhang, Zn(II)-Containing Metal-Organic Framework for Fluorescence Detection of Nitrobenzene and Prevention Effect on Hypertension via Down-Regulating the Expression of Vitamin D Receptor, *J. Clust. Sci.* 31 (2020) 479–486.
- [59] K.S. Asha, K. Bhattacharyya, S. Mandal, Discriminative detection of nitro aromatic explosives by a luminescent metal-organic framework, *J. Mater. Chem. C*. 2 (47) (2014) 10073–10081.
- [60] S. Xian, H.L. Chen, W.L. Feng, X.Z. Yang, Y.Q. Wang, B.X. Li, Eu(III) doped zinc metal organic framework material and its sensing detection for nitrobenzene, *J. Solid. State. Chem.* 280 (2019) 47–52.
- [61] H. He, S.-H. Chen, D.-Y. Zhang, E.-C. Yang, X.-J. Zhao, A luminescent metal-organic framework as an ideal chemosensor for nitroaromatic compounds, *Rsc. Adv.* 7 (62) (2017) 38871–38876.
- [62] X. Luo, X. Zhang, Y.L. Duan, X.L. Wang, J.M. Zhao, A novel luminescent Pb(II)-organic framework exhibiting rapid and selective detection of trace amount of NACs and Fe^{3+} with excellent recyclability, *Dalton Trans.* 46 (2017) 6303–6311.
- [63] G.-Y. Wang, L.-L. Yang, Y. Li, H. Song, W.-J. Ruan, Z.e. Chang, X.-H. Bu, A luminescent 2D coordination polymer for selective sensing of nitrobenzene, *Dalton Trans.* 42 (36) (2013) 12865, <https://doi.org/10.1039/c3dt51450a>.
- [64] R.X. Yao, X. Cui, X.X. Jia, F.Q. Zhang, X.M. Zhang, A luminescent zinc(II) metal-organic framework (MOF) with conjugated pi-electron ligand for high iodine capture and nitro-explosive detection, *Inorg. Chem.* 55 (2016) 9270–9275.